

Multipole collectivity in ^{168}Er from inelastic scattering

I. M. Govil, H. W. Fulbright, D. Cline, E. Wesolowski,* B. Kotlinski,* A. Backlin,[†] and K. Gridnev[‡]
Nuclear Structure Research Laboratory, University of Rochester, Rochester, New York 14627

(Received 15 October 1985)

The structure of the low-lying states of ^{168}Er has been investigated by use of inelastic scattering. Differential cross sections for the elastic and inelastic scattering of 36 MeV α particles and 16 MeV deuterons from ^{168}Er have been measured. Isoscalar transition strengths for $l=2, 3$, and 4 excitation have been extracted by a coupled-channels distorted wave calculation involving collective model form factors. A number of known levels corresponding to the ground state band, γ band, and octupole bands were seen. Results for the 2^+ , 4^+ , 6^+ , and 8^+ states in the ground state band and 2^+ , 4^+ , and 6^+ states in the γ band imply the importance of the hexadecapole (β_4) and the hexacontatetrapole (β_6) shape components. The octupole states at 1431, 1633, and 1913 keV are excited with isoscalar strengths equal to 0.046, 0.058, and 0.023 e^2b^3 , respectively, which are comparable with the corresponding $B(E3)$ strengths known from Coulomb excitation of the 1431 and 1633 keV states. The octupole states at 2269, 2324, and 2486 keV with isoscalar $E3$ transition strengths 0.055, 0.022, and 0.018 e^2b^3 , respectively, are newly identified. For quadrupole excitation the results agree in several ways with predictions of the interacting boson approximation model and the geometrical models and for octupole states there is a good agreement with theoretical results of Neergård and Vogel.

I. INTRODUCTION

The properties of the low-lying states in ^{168}Er , and many other strongly deformed nuclei, are characteristic of collective rotation of an axially symmetric, quadrupole-deformed nucleus. The establishment of a detailed level scheme including 20 collective bands for the heavy deformed nucleus ^{168}Er by Davidson *et al.*¹ on the basis of (n,γ) resonance measurements led to theoretical calculations on the basis of both the interacting boson model² (IBA) and the conventional Bohr-Mottelson model.³ Comparisons^{2,3} of the results from these models were made using the known energy level spectrum and γ -ray branching ratios.¹ A more recent comparison⁴ shows that the geometrical models of the collective excitation give results similar to those of the IBA model. The difference between the results of the calculations of Refs. 2 and 3 probably reflects more the restrictions used in the calculations than the deficiencies in the models.

The present study of inelastic alpha and deuteron scattering was initiated to find absolute $l=2, 3$, and 4 isoscalar transition strengths $B(\text{IS};l)$, since these are especially sensitive to l multipole collectivity, and hence can provide a stringent test of collective models. A parallel study of heavy-ion induced Coulomb excitation⁵ also was made to obtain a more detailed study of the electric quadrupole properties. In the present experiments, the $^{168}\text{Er}(\alpha,\alpha')$ and $^{168}\text{Er}(d,d')$ reactions have been studied with 36 MeV α particles and 16 MeV deuterons. The data have been analyzed by exploiting the formal similarity between electromagnetic and inelastic scattering transition strengths outlined by Bernstein.⁶ The greater part of the experimental effort was devoted to (α,α') work; the (d,d') experiments were intended to provide corroborating information.

II. EXPERIMENTAL DETAILS

The experiments were done with 36 MeV alphas and 16 MeV deuterons from the 13 MV tandem Van de Graaff accelerator at the Nuclear Structure Research Laboratory of the University of Rochester. The reaction products were analyzed with an Enge split-pole magnetic spectrometer, with a position-sensitive proportional counter in the focal plane. This detector comprises a 0.3 mm resolution position-sensitive section followed by two conventional proportional counters which could be used in coincidence. The targets were 50–100 $\mu\text{g}/\text{cm}^2$ of ^{168}Er evaporated onto 20 $\mu\text{g}/\text{cm}^2$ carbon foils. The beam was carefully aligned and often no entrance slit was used in the scattering chamber in order to minimize the background due to slit scattering. The overall energy resolution was roughly 18 keV for 36 MeV scattered alphas and 10 keV for 16 MeV scattered deuterons. The angular range of observation was in steps of 5° from 20° to 70° for α particles and 35° to 105° for deuterons. With α particles it was in general possible to secure an internal normalization by recording simultaneously both elastic and inelastic scattering. Normalization information was also obtained by monitoring the scattering at 45° with a solid state detector for α particles and a NaI (Tl) scintillator for deuterons. Absolute cross sections were obtained by normalizing to forward-angle elastic scattering data. The background associated with the tail of the elastic scattering peak and with elastic and inelastic scattering from impurities—particularly C, O, and Si—sometimes interfered significantly, especially at small scattering angles.

A spectrum for the scattering of α particles at 60° is shown in Fig. 1. The centroids of the peaks are located with an accuracy of ± 5 keV. Shown in Fig. 2 is the level energy diagram of Davidson *et al.*¹ A moderate number

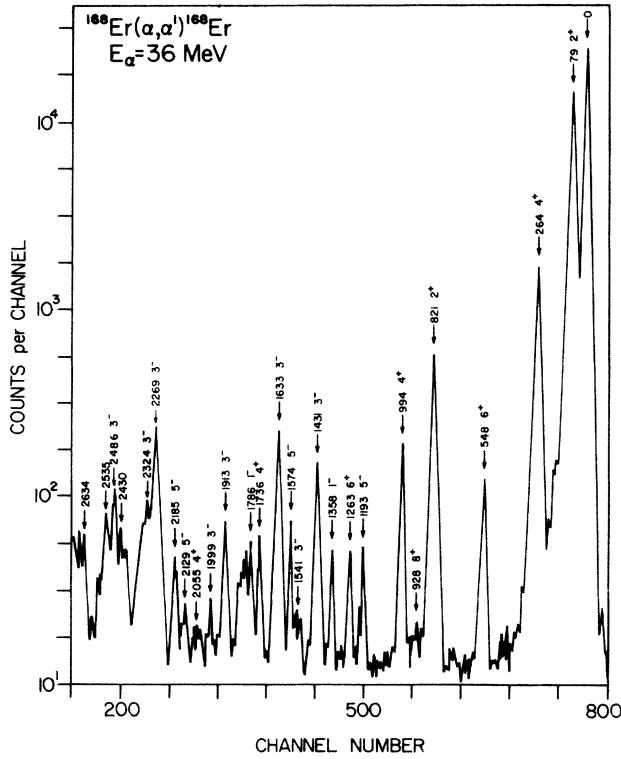


FIG. 1. A spectrum of scattered α particles at 60° .

of the many known low-spin natural parity levels are seen strongly enough to be identified. Thick solid lines in Fig. 2 indicate the strongly excited states and the thick broken lines the relatively weakly excited states in the present experiment. The states excited include all members of the ground state band through 8^+ , the 2^+ , 4^+ , and 6^+ members of the $K=2^+$ (γ) band beginning at 821 keV, the 1431 keV 3^- member of the $K=1^-$ band beginning at 1358 keV, the 1633 keV 3^- member of the $K=2^-$

band beginning at 1569 keV, and the 1913 keV 3^- member of the $K=0^-$ band beginning at 1786 keV. Careful observations with both α 's and deuterons failed to show evidence for the proposed β band (second $K=0^+$); neither the 1217 keV 0^+ nor the 1276 keV 2^+ level appeared above the background, so an upper limit for the $B(E2)$ value of the 1276 keV transition can be set. In addition to the states shown in Fig. 2, states at 2269, 2324, 2430, 2486, 2535, and 2634 keV were excited with appreciable cross section.

At large angles the angular distributions for both α particles and deuterons were found to be relatively structureless. However, for $\theta \leq 35^\circ$ the angular distributions are sensitive to the multipolarity of excitation as shown later.

III. ANALYSIS

A. Ground state and γ bands

The angular distributions for the ground state and the γ band have been analyzed using the coupled channels code ECIS79 (Ref. 7) (henceforth called simply ECIS). The complex optical-model potential has the Woods-Saxon form with volume and surface absorption to which the Coulomb potential is added, i.e.,

$$V(r, \theta', \phi') = -(V + iW)(1 + e)^{-1} - 4iW_s e(1 + e)^{-2} + V_{\text{Coul}} \quad (3.1)$$

with

$$e = \exp\{[r - R(\theta', \phi')]/a\} \quad (3.2)$$

The ground band properties in ^{168}Er , and many other strongly deformed nuclei, are reproduced well using the Bohr-Mottelson model of collective rotation of an axially-symmetric quadrupole-shaped nucleus. An adequate description of the γ band and hexadecupole excitation requires extension of the simplest rotational model to include the influence of the triaxial quadrupole deforma-

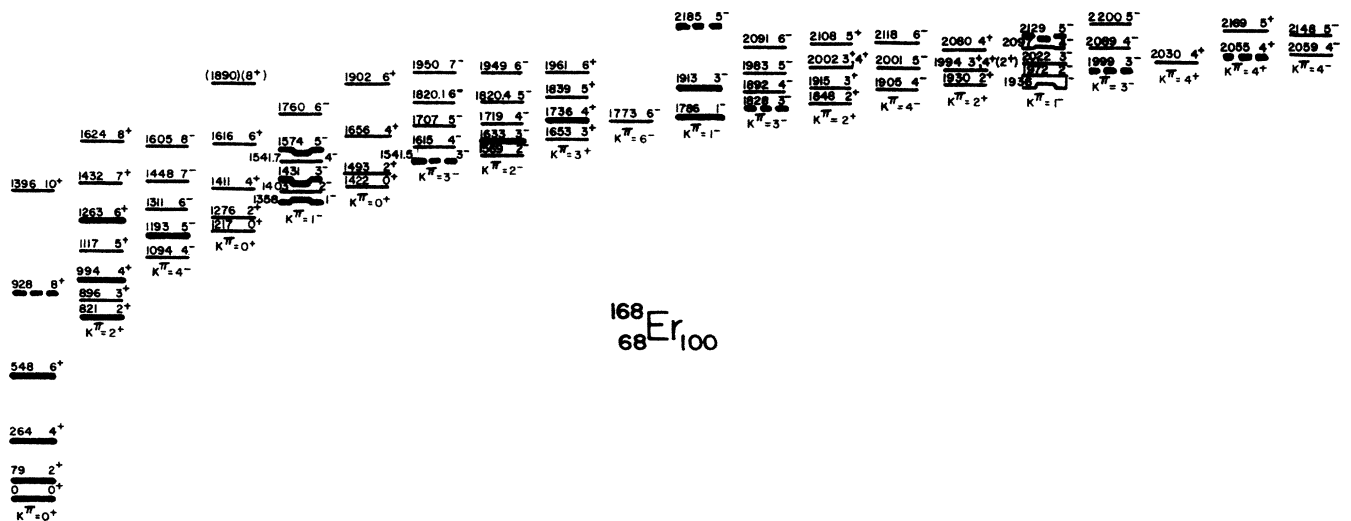


FIG. 2. Energy level diagram proposed by Davidson *et al.* (Ref. 1) from the (n, γ) resonance measurement. Thick solid lines show strongly populated states and broken lines show weakly populated states in the present experiment.

tion and hexadecupole degrees of freedom. The interpretation of the γ degrees of freedom is a long-standing problem. Bohr and Mottelson³ have described this collective motion as a quadrupole shape oscillation with some rms γ value about an axially symmetric equilibrium shape, whereas Davydov and Filippov⁸ assumed it to be due to collective rotation of a rigid triaxially-deformed quadrupole shape with fixed γ value. A description somewhere between these two extremes probably would be better.

$$R(\theta', \phi') = R_0 [1 + \beta_2 \cos(\gamma) Y'_{2,0} + (1\sqrt{2})\beta_2 \sin(\gamma) Y'_{2,\pm 2} + \beta_4 Y'_{4,0} + (1\sqrt{2})\beta_4 Y'_{4,\pm 2} + (1\sqrt{2})\beta_4 Y'_{4,\pm 4} + \beta_6 Y'_{6,0} + (1\sqrt{2})\beta_6 Y'_{6,\pm 2} + \beta_8 Y'_{8,0}] . \quad (3.3)$$

The prime attached to the surface harmonics $Y'_{\lambda k}$ means that their arguments are polar angles referred to the body fixed coordinate system. The simple Davydov and Filippov^{8,9} model was used to calculate the wave function for the states of interest. That is, the nuclear states were expanded in terms of the axially symmetric eigenfunctions

$$|IM; \alpha\rangle = \sum_K A_{\alpha K}^I |IMK\rangle , \quad (3.4)$$

where

$$|IMK\rangle = \left[\frac{2I+1}{16\pi^2(1+\delta_{K0})} \right]^{1/2} [D_{M,K}^I + (-)^J D_{M,-K}^I] . \quad (3.5)$$

The band mixing coefficients $A_{\alpha K}^I$ were determined using the eigenequation

$$\sum_{K'} \langle IMK' | H_{\text{rot}} | IMK \rangle A_{\alpha K'}^I = E_{\alpha}^I A_{\alpha K}^I , \quad (3.6)$$

where the rotational Hamiltonian is

$$H_{\text{rot}} = \sum_{i=1}^3 \frac{J_i^2}{2\mathcal{I}_i} . \quad (3.7)$$

The three moments of inertia \mathcal{I}_i were calculated to best reproduce the level energies of the 2^+ states of the ground and the γ band in ^{168}Er . The band mixing coefficients or parameters $A_{\alpha K}^I$ determined by the solution of equation (3.6) were included in the asymmetric rotor model ECIS calculations.

B. Octupole vibrational states

The nucleus ^{168}Er has a strongly deformed ground state, therefore the analysis of 3^- states in this nucleus has been done in the framework of octupole vibrations of an axially symmetric and statically deformed nucleus. Since ECIS does not have any built in provision to calculate form factors for this model we have calculated them using the prescription given by Tamura.^{10,11} The nuclear potential between target and projectile is assumed to be the Woods-Saxon form (3.1) with the radius parameter given in the body-fixed frame of reference by

Fortunately, for the small value of the quadrupole asymmetry parameter $\gamma \approx 9^\circ$ occurring in ^{168}Er , these two limiting descriptions lead to essentially identical results for the properties studied in the present paper. The present data were analyzed via the rigid triaxial rotor model, and extended to include hexadecupole and higher multipole deformations. The inelastic scattering data were analyzed with the radial shape (in the body fixed frame of reference) given by

$$R(\theta', \phi') = R_0 \left[1 + \sum_l \beta_l Y'_{l0} + \sum_{\lambda K} \beta_{\lambda K} Y'_{\lambda K} \right] . \quad (3.8)$$

The statically symmetric shape is given by the sum over l and the dynamical axial and nonaxial terms are given by a sum over λ and K . In our analysis we have limited the static deformation to $l=2$ and 4 and the dynamic deformation is taken to be $\lambda=3$ corresponding to the octupole vibration only. The small nonaxial static deformation ($\gamma=9^\circ$) present in this nucleus has not been included since its effect on the 3^- states is estimated to be negligible. Therefore, $R(\theta', \phi')$ may be written as

$$R(\theta', \phi') = R_0 \left[1 + \beta_2 Y'_{20} + \beta_4 Y'_{40} + \sum_K \beta_{3K} Y'_{3K} \right] . \quad (3.9)$$

The angular coordinate θ' is in the body-fixed system. For ease of calculation (3.9) and (3.2) are inserted in (3.1) and the latter is expanded in first order of β_{3K} by Taylor series with the result

$$V(r, \theta', \phi') = V_1(r, \theta') + \sum_K \beta_{3K} V_2(r, \theta') Y'_{3K} . \quad (3.10)$$

$V_1(r, \theta')$ is the same as (3.1) with (3.2) and (3.9) except that $\beta_{3K}=0$, while $V_2(r, \theta')$ is given by

$$V_2(r, \theta') = -(V+iW) \left[\frac{R_0}{a} \right] e(1+e)^{-2} - 4iWs \left[\frac{R_0}{a} \right] e(e-1)(1+e)^{-3} , \quad (3.11)$$

where e is given by (3.2) and (3.9) with $\beta_{3K}=0$

The potentials V_1 and V_2 in (3.10), which are still functions of β_2 and β_4 , are expanded in terms of the spherical harmonics with the result

$$V(r, \theta', \phi') = \sum_l v_l^{(1)}(r) Y'_{l0} + \sum_K \beta_{3K} \sum_l v_l^{(2)}(r) Y'_{l0} Y'_{3K} , \quad (3.12)$$

where

$$v_l^{(1)}(r) = 4\pi \int_0^1 V_1(r, \theta') Y_{l0} d(\cos\theta') \quad (3.13)$$

and

$$v_l^{(2)}(r) = 4\pi \int_0^1 V_2(r, \theta') Y_{l0} d(\cos\theta') ; \quad (3.14)$$

by using the general formula for the coupling of angular momentum¹² we may write (3.12) as

$$V(r, \theta', \phi') = \sum_l v_l^{(1)}(r) Y_{l0}' + \sum_{\lambda K} \tilde{v}_{\lambda K}^{(2)}(r) Y_{\lambda K}'(\theta', \phi'), \quad (3.15)$$

where

$$\tilde{v}_{\lambda K}^{(2)}(r) = \beta_{3K} \sum_{l=0,2,4} v_l^{(2)}(r) \left[\frac{7(2l+1)}{4\pi(2\lambda+1)} \right]^{1/2} \times \langle 1030 | \lambda 0 \rangle \langle 103K | \lambda K \rangle. \quad (3.16)$$

In Eq. (3.15) we replace $Y_{\lambda K}'$ by $\sum_{\mu} D_{\mu K}^{\lambda} Y_{\lambda \mu}(\theta, \phi)$, where θ and ϕ are the polar angles that refer to the space-fixed coordinate system. Hence the final form of the optical potential to be used in the present coupled channel calculations is given by

$$V(r, \theta, \phi) = \sum_{l\mu} v_l^{(1)} D_{\mu 0}^l Y_{l\mu}(\theta, \phi) + \sum_{\lambda\mu} \tilde{v}_{\lambda K}^{(2)}(r) D_{\mu K}^{\lambda} Y_{\lambda \mu}(\theta, \phi). \quad (3.17)$$

The first part connects states of the same rotational band, while the second part gives the transition from ground state band to the members of other rotational bands built on the octupole vibrational states with $K=0, 1, 2, 3$, etc.

The octupole vibration introduces a spurious center of mass motion for which a correction term¹³ is added to (3.9) so that the final form factor is given by

$$\tilde{v}_{\lambda K}^{(2)}(r) = \sum_{l=0,2,4} v_l^{(2)}(r) \left[\frac{7(2l+1)}{4\pi(2\lambda+1)} \right]^{1/2} \times (\beta_{3K} \langle 1030 | \lambda 0 \rangle \langle 103K | \lambda K \rangle - \epsilon_{\mu} \langle 1010 | \lambda 0 \rangle \langle 101K | \lambda K \rangle). \quad (3.18)$$

The ϵ_{μ} is not an independent variable but its value is fixed in terms of β_{3K} by the condition of translation invariance, i.e.,

$$\int \tilde{v}_{\lambda=1}^{(2)}(r) r^3 dr = 0. \quad (3.19)$$

The coupled channel calculations have been done with the use of ECIS;⁷ the form factors (3.18) for the interband transitions have been calculated externally and fed to the program along with the relevant reduced nuclear matrix elements.

IV. INELASTIC SCATTERING CROSS SECTION AND ISOSCALAR TRANSITION STRENGTH

The inelastic scattering of α particles and deuterons is a powerful spectroscopy probe because, for these strongly

absorbed projectiles at the bombarding energies used here, the inelastic transition density is peaked at the nuclear surface, as is the electromagnetic $E\lambda$ transition density. Consequently, the inelastic scattering transition strengths are closely related to the isoscalar part of the corresponding electromagnetic $B(E\lambda)$ values and are insensitive to the exact details of the collective model and the optical model parameters used in the reaction mechanism. Bernstein⁶ defined an inelastic scattering isoscalar transition strength which is similar to the isoscalar part of the corresponding electromagnetic $B(E\lambda)$ and developed a method for extracting it from inelastic scattering data. The close agreement between the inelastic isoscalar transition strengths and corresponding $B(E\lambda)$ has been demonstrated in the past¹⁴ and is found to occur in the present work.

According to Bernstein⁶ the inelastic transition matrix element is defined as

$$T^{lm}(\theta) = \langle \psi_f(r) | \sum_{\text{nucleons}} O^{lm}(\theta, r) Y_{lm}(\Omega) | \psi_i(r) \rangle, \quad (4.1)$$

where ψ_i and ψ_f are the nuclear wave functions for the initial and final states, and the transition operator $O^{lm}(\theta, r)$ is given by

$$O^{lm}(\theta, r) = \langle \psi^{(-)}(k_f, r_{\alpha}) | V_l(r, r_{\alpha}) Y_{lm}^*(\Omega_{\alpha}) | \psi^{(+)}(k_i, r_{\alpha}) \rangle. \quad (4.2)$$

The incoming wave $\psi^{(-)}$ and the outgoing wave $\psi^{(+)}$ are the solutions of the Schrödinger equation for the projectile in the presence of the α -nucleon interaction $V_l(r, r_{\alpha})$. The behavior of the function $O^l(r)$ has been investigated thoroughly by Bernstein and found to be qualitatively similar to r^l , both favoring the surface region. This similarity leads one to define an isoscalar multiple operator $O(\text{IS})$ similar to the electromagnetic transition operator; thus

$$O(\text{IS}) = Z/A \sum_{\text{nucleons}} r^l Y_{lm}(\Omega). \quad (4.3)$$

The scaling factor Z/A is introduced for convenience so that if the relative neutron to proton contribution to the IS transition operator is in the ratio N/Z , then the IS and electromagnetic (EM) transition rates will be numerically equal. Within the collective model the isoscalar matrix elements can be written in terms of the mass density distribution $\rho(r)$ as¹⁵

$$[B(\text{IS } l, 0 \rightarrow l)]^{1/2} = M(\text{IS}) = \frac{Z}{A} \int r^l Y_{lm}(\Omega) \rho(r) dr. \quad (4.4)$$

If the mass and charge distribution of the ground state are assumed to be of the same form as of the nuclear potential then

$$\rho(r) = \rho_0 \left\{ 1 + \exp \left[\frac{r - R(\theta, \phi)}{a} \right] \right\}^{-1}, \quad (4.5)$$

where $R(\theta, \phi)$ is given by Eq. (3.3) and ρ_0 is fixed by the constraint that the total number of nucleons is conserved.

In case of static deformation the reduced IS transition

strength may be obtained directly by numerical integration of Eq. (4.4), while in case of nonstatic deformation, the deformation parameter is comprised of the destruction and creation operators for a 2^1 -pole vibration; hence in such a case a Taylor series expansion about $R = R_0$ yields to second order

$$\rho(r) = \rho(r - R_0) + (\delta R) \left[\frac{d}{dR_0} \right] \rho(r - R_0) + \frac{1}{2} (\delta R)^2 \left[\frac{d^2}{dR_0^2} \right] \rho(r - R_0), \quad (4.6)$$

where

$$\delta R = R - R_0 = R_0 \sum_{\lambda k} \beta_{\lambda k} Y_{\lambda k}(\theta, \phi).$$

Insertion of Eq. (4.6) into (4.4) leads to

$$[B(\text{IS } l, 0 \rightarrow l)]^{1/2} = M(\text{IS } l, K) = \frac{Z}{A} (\beta_{lm} X_l + B_{lm} Z_l), \quad (4.7)$$

where

$$X_l = R_0 \int \left[\frac{d\rho}{dR_0} \right] r^{l+2} dr, \quad (4.8)$$

$$Z_l = \frac{1}{2} R_0^2 \int \left[\frac{d^2\rho}{dR_0^2} \right] r^{l+2} dr, \quad (4.9)$$

and

$$B_{lm} = \sum_{\lambda\lambda'K} \beta_{\lambda K} \beta_{\lambda'm-K} \left[\frac{(2\lambda+1)(2\lambda'+1)}{4\pi(2l+1)} \right]^{1/2} \times \langle \lambda K \lambda' m - K | lm \rangle \langle \lambda 0 \lambda' 0 | l 0 \rangle. \quad (4.10)$$

Note that B_{lm} will be zero unless $\lambda + \lambda' + l = \text{even}$. The value of deformation parameters β_2 and β_4 , etc., along with their components in case of static deformation and β_{3K} in case of dynamic octupole vibration, are obtained by comparing the experimental cross sections with the theoretical values as discussed in Secs. III A and III B. These values are used to calculate the isoscalar matrix elements or transition strengths $B(\text{IS } l)$ by the use of Eqs. (4.4) and (4.7). The extracted deformation parameters β_2 , γ , β_{40} , β_{42} , β_{44} , β_{60} , β_{62} , and β_8 are highly model dependent while the corresponding $B(\text{IS})$ are considerably less so, and are less dependent on the parameters characterizing the reaction mechanism.

V. RESULTS AND DISCUSSION

A. Transition strengths for even multipoles

The measured and calculated angular distributions for elastic and inelastic α scattering of the 2^+ , 4^+ , 6^+ , and 8^+ states of the ground state band and the 2^+ , 4^+ , and 6^+ states of the γ band are shown in Figs. 3–5. The values of the optical potential parameters obtained by least squares fitting to the elastic scattering cross section data are given in Table I. The parameters

(V_0 , V_w , r_0 , a_0 , etc.) were varied in an automatic fitting procedure using as starting values the parameters from an earlier study of 50 MeV α particle scattering on ^{166}Er by Hendrie *et al.*¹⁶ The deformation parameters β_2 – β_8 were derived by comparing the inelastic cross section with the theoretical values in a self-consistent way. First, a rough value of β_2 was calculated by comparing the inelastic scattering data of the first 2^+ state with the rotational model calculations using only transitions between the ground state and 2^+ state. The 4^+ state was then introduced and a search was made on β_2 and β_4 simultaneously, and so on, as higher states were introduced in the calculation. The deformation and asymmetry parameters

$$\beta_2 = +0.23 \pm 0.01,$$

$$\gamma = 9^\circ,$$

$$\beta_{40} = -0.021_{-0.009}^{+0.025},$$

$$\beta_{42} = +0.023 \pm 0.002,$$

$$\beta_{44} = \pm 0.008 \pm 0.002,$$

$$\beta_{60} = -0.0091 \pm 0.0012,$$

and

$$\beta_{62} = +0.0072 \pm 0.0008$$

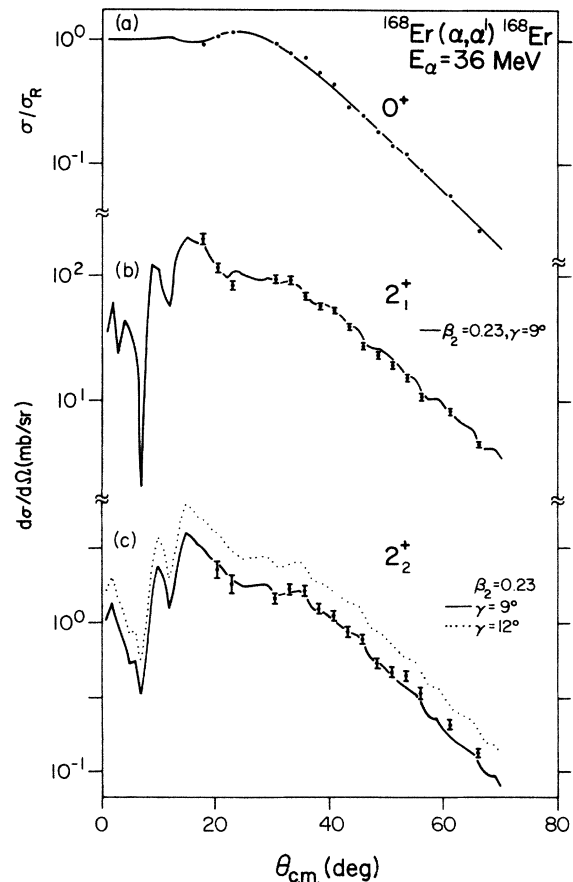


FIG. 3. Experimental data and the asymmetric rotor model coupled channel results for (α, α') reactions at $E_\alpha = 36$ MeV. (a) 0^+ (g.s.), (b) 2_1^+ (79 keV) state, and (c) 2_2^+ (821 keV) state.

were derived by comparing the experimental cross sections with the asymmetric rotor model calculations. Included in the final asymmetric model ECIS calculations were transitions to the following states: 2_1^+ (79 keV), 2_2^+ (821 keV), 3_1^+ (896 keV), 4_1^+ (264 keV), 4_2^+ (994 keV), 4_3^+ (2055 keV, $K=4^+$), 5_1^+ (1117 keV), 6_1^+ (548 keV), and 6_2^+ (1263 keV). Figure 5(c) shows the results for the symmetric rotor model ECIS calculation for the 8_1^+ state of the ground state band. The peak for this state was resolved only at a few higher angles and the results indicate the value of $\beta_{80} \leq |0.01|$.

Shown in Fig. 6 are the elastic and inelastic cross sections from the (d,d') reaction at 16 MeV using the optical potential parameter given in Table I. The starting values of the parameters in this case were taken from the global parameters of Daehnick *et al.*¹⁷ The value of

$$\bar{\beta}_2(R_0\beta_2/1.2) = 0.276,$$

corrected for the radius of the real potential and derived from the cross section of the first 2^+ state in the present (d,d') experiment, agrees with the value from our (α,α') experiment, which also agrees with the $\bar{\beta}_2$ value obtained

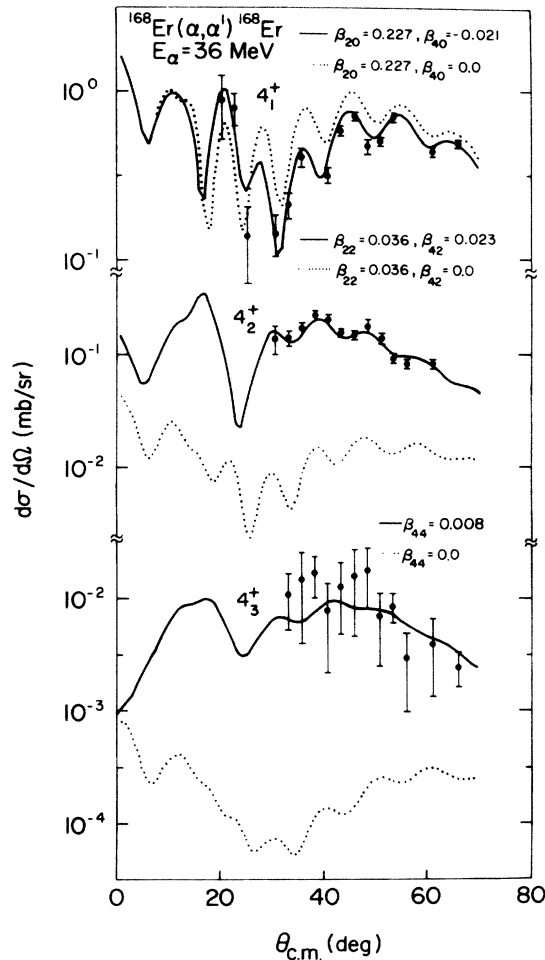


FIG. 4. Experimental data and the asymmetric rotor model coupled channel results for (α,α') reactions at $E_\alpha=36$ MeV. (a) 4_1^+ (264 keV) state, (b) 4_2^+ (994 keV) state, and (c) 4_3^+ (2055 keV, $K=4^+$) state.

by Hendrie *et al.*¹⁶ for ^{166}Er using 50 MeV α particles. This indicates that the β_2 values or transition strengths so derived are insensitive to the energy and type of the projectile.

The γ value $=9^\circ$ agrees with the value $(\langle\gamma^2\rangle)^{1/2}=9^\circ$ derived by Bohr and Mottelson³ from the Coulomb excitation $B(E2)$ values.⁵ Although it disagrees with the value $\gamma=12^\circ$ deduced from the relative spacing of the first two 2^+ states,⁸ there is no *a priori* reason why the asymmetries derived from level energy systematics and from transition strengths must be the same. Bohr and Mottelson derived the rms γ -vibration amplitude of the symmetric deformed nuclei while our calculations assume a triaxial nuclear equilibrium shape. Nevertheless, for such

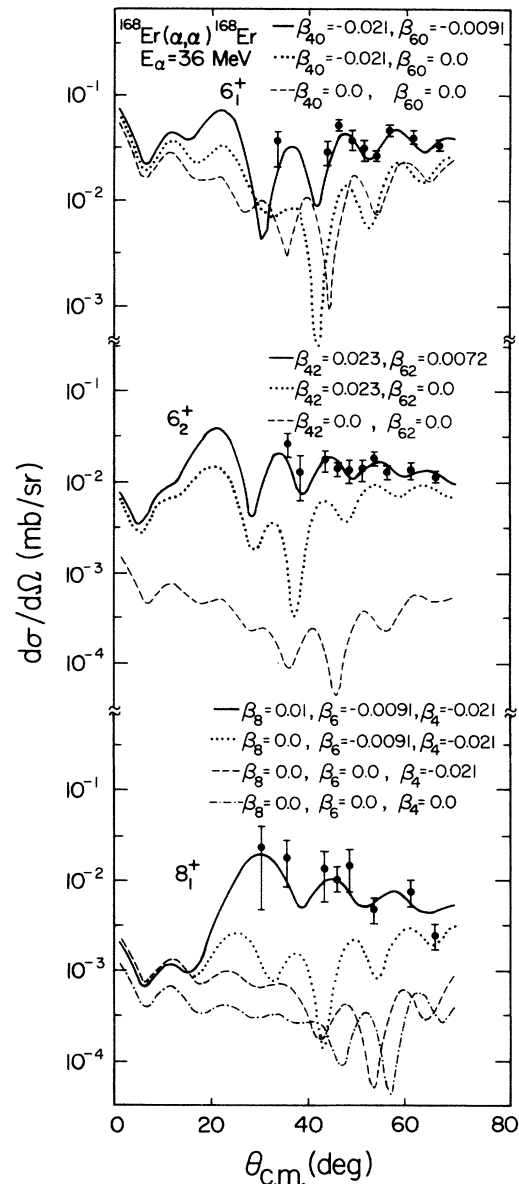


FIG. 5. Experimental data and the asymmetric rotor model coupled channel results for (α,α') reactions at $E_\alpha=36$ MeV. (a) 6_1^+ (548 keV) state, (b) same for the 6_2^+ (1263 keV) state, and (c) the symmetric rotor model coupled channel results for the 8_1^+ (928 keV) state.

TABLE I. Optical model potential parameters.

Reaction (projectile energy)	Deformed volume Real			Deformed ^a volume Imaginary			Deformed ^a surface Imaginary			Deformed ^a Coulomb		Deformed ^a spin-orbit Real		
	V_0 (MeV)	r_0 (fm)	a_0 (fm)	V_w (MeV)	r_w (fm)	a_w (fm)	V_s (MeV)	r_s (fm)	a_s (fm)	r_c (fm)	a_c (fm)	V_{LS} (MeV)	r_{LS} (fm)	a_{LS} (fm)
$^{168}\text{Er}(\alpha, \alpha')$ (36 MeV)	64.28	1.44	0.616	29.44	1.52	0.418	0.9	1.52	0.418	1.52	0.418			
$^{168}\text{Er}(d, d')$ (16 MeV)	94.32	1.166	0.83	0.316	1.368	0.878	12.18	1.368	0.878	1.30	0.0	6.69	1.07	0.508

^aThe deformation parameters are normalized to the radius of the volume real potential.

small values of γ it is difficult to distinguish between these two cases. The finite values of β_{40} , β_{42} , and β_{44} needed for a reasonable fit to the 4_1^+ , 4_2^+ , and 4_3^+ states show the importance of the $\Delta K \neq 0$ components for the hexadecupole deformation as reported earlier by us¹⁸ and verified recently by Ichihara *et al.*¹⁹ via (p,p') work. The fits (Fig. 5) to the 6_1^+ and 6_2^+ states also show relatively large β_{60} and β_{62} components in this nucleus. Our value $\beta_{42} = 0.023 \pm 0.002$ ($R_0 = 1.44$) agrees with the Ref. 19 value of $\beta_{42} = 0.0258$ ($R_0 = 1.224$), if scaled to the same radius of the real potential. Our values of $\beta_{40} = -0.021 \pm 0.025$ and $\beta_{60} = -0.0091 \pm 0.0012$ are slightly different from their values of $\beta_{40} = -0.0087$ and $\beta_{60} = -0.0197$. The χ^2 curve for the 4_1^+ has a broad minimum with the lowest value at $\beta_{40} = -0.021$. The large uncertainty in β_{40} from -0.012 to -0.046 causes the matrix element $M(E4)$ to change from $+0.157$ to -0.188 . The Coulomb excitation³² results give a positive value of $M(E4) = +0.179 \pm 0.054$ corresponding to $\beta_{40} = -0.01 \pm 0.005$ which is consistent with the results of the present work within experimental errors. The slope of the curve for the 4_3^+ favors a positive value of β_{44} , but due

to the large error in experimental data for this state, a negative value of β_{44} may also not be ruled out. Note that the K mixing for the three lowest 4^+ states is predicted to be negligible by the Davydov-Filippov model. Consequently the values of β_{40} , β_{42} , and β_{44} came directly from the cross sections to the 4^+ states of the $K=0, 2$, and 4 bands, respectively.

Table II gives a comparison of the isoscalar transition strength derived from the present experiments with electromagnetic transition strengths obtained from Coulomb excitation experiments and various geometrical collective and IBA model predictions. The table also gives the $G(\text{IS})$ values, i.e., the transition rates in single particle units

$$B_{\text{s.p.}}(El, 0 \rightarrow l) = \frac{(2l+1)}{4\pi} \left[\frac{3}{3+l} \right]^2 (r_0 A^{1/3})^{2l}. \quad (5.1)$$

The IBA estimates in the table are derived using as $E2$ and $E4$ operators

$$T(E2) = E2SD(s^\dagger \tilde{d} + d^\dagger \tilde{s})^2 + (1/\sqrt{5})E2DD(d^\dagger \tilde{d})^2 \quad (5.2)$$

and

$$T(E4) = (1\sqrt{9})E4DD(d^\dagger \tilde{d})^4. \quad (5.3)$$

Values of the constants $E2SD$, $E2DD$, and $E4DD$ are selected to reproduce the IS transition rates of 2_1^+ , 2_2^+ , and 4_1^+ states. The assumed ratio $E2DD/E2SD = -0.68$ lies between the pure SU_3 limit (-2.958) and the γ -unstable $0(6)$ limit (zero). The perturbed SU_3 Hamiltonian is that suggested by Warner *et al.*²

The isoscalar transition rates and the EM transition rates listed in Table II agree within experimental errors. For the 2_3^+ state of the so-called β -vibration band our transition strength is closer to the Bohr-Mottelson value than to the other geometrical models and is a factor of 4 larger than the IBA value. The IBA model underpredicts the strength of the $0_1^+ \rightarrow 4_2^+$ transition by a factor of 40, but this result may in part be due to neglect of g-boson contributions to $T(E4)$.

B. The octupole transition strengths

Some of the 3^- states in ^{168}Er have been observed earlier in nuclear reactions,²⁰⁻²² but the results were not

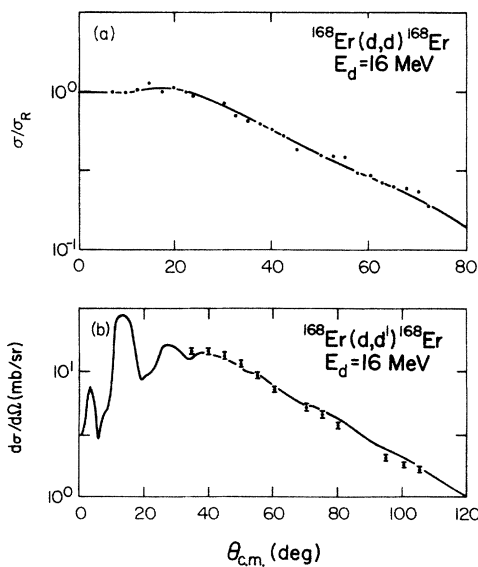


FIG. 6. Experimental data and the coupled channel results for the (d,d') reaction at $E_d = 16$ MeV. (a) 0^+ (g.s.) and (b) 2_1^+ (79 keV) state.

analyzed in detail. Tjøm and Elbek²⁰ derived $B(\text{IS3})$ values from (d,d') experiments performed using 12 MeV deuterons. McGowan *et al.*²³ have measured $B(E3)$ values of the 1431 and 1634 keV states on the basis of Coulomb excitation with 14 MeV α particles. However, their ratio of $E1$ transition strengths from the 1431 keV 3^- state to the 2^+ and 4^+ members of the ground state band are in closer agreement with the Alaga prediction²⁴ for $K=0^-$ rather than for the $K=1^-$ band. Michaelis *et al.*²¹ have predicted earlier that this state belongs to a $K=1^-$ band, which has been confirmed recently by Davidson *et al.*¹ on the basis of $E1$ multipolarities of transitions to the ground state band. We have, therefore, assumed the 1431 keV state to be a member of the $K=1$ band. The 1633 and 1913 keV 3^- states observed in our experiments are assumed to belong to predominantly $K=2^-$ and $K=0^-$ bands, respectively. However, as pointed out in Ref. 27 the Coriolis interaction may cause large K admixture for the low lying 3^- states.

The results of the coupled-channel calculations based on the model discussed earlier in this paper are shown in Fig. 7. The couplings assumed in the calculations are

shown in the insert of each diagram. Also shown in the figure are the DWBA results for direct one-step excitation from the ground state. The optical potential parameters used in all these calculations are listed in Table I. The deformation strengths β_{3K} are derived for each 3^- state from the best fit to the experimental data using the automatic search feature of ECIS.

It is evident from Fig. 7 that the simple DWBA results do not fit the experimental angular distribution. Also shown in the figure are the predictions (dashed curve) if the quadrupole moment of the 3^- states or the reorientation matrix element is assumed to be zero. A similar sensitivity to the assumed quadrupole moments was reported earlier²⁵ in the case of ^{148}Nd .

Data for the relatively strongly excited states at 2269, 2324, and 2486 keV, not previously identified, were analyzed in the framework of octupole or quadrupole vibration of an axially symmetric and statically deformed nucleus with $\beta_2=0.23$ on the assumption of $J^\pi=2^+$ or 3^- . The angular distributions shown in Fig. 8 are found to be consistent with the assignment 3^- rather than 2^+ for these states.

TABLE II. Comparison of the present isoscalar (IS) transition rates with the electromagnetic (EM) transition rates, various geometrical collective models, and the interacting boson model (IBA).

Transition	Energy (keV)	$E1$	$G(\text{IS})$ (s.p.u.)	Present		Coulomb excitation	Geometrical models (theory)	IBA model (theory)
				$B(\text{IS})^a$ (e^2b^4)	$B(\text{EM})$ (e^2b^4)	$B(E2)$ (e^2b^4)	$B(\text{IBA})$ (e^2b^4)	
$0 \rightarrow 2_1^+$	79	$E2$	250.9	6.8(9)	5.77(8) ^c 5.92(10) ^d	5.77 ^c	5.77 ^c	
$0 \rightarrow 2_2^+$	821	$E2$	4.7	0.136(15)	0.131(8) ^e 0.130(5) ^f 0.137(9) ^g	0.124(BM) ^k	0.137	
$0 \rightarrow 2_3^+$	1276	$E2$	≤ 0.1	≤ 0.002		0.0016(BM) ^k 0.0435(GGM) ^l 0.111(GCM) ^l 0.208(RVM) ^l	0.00044	
$0 \rightarrow 4_1^+$	264	$E4$	3.9	0.004(35)	0.032(20) ^h 0.053($^{+70}_{-47}$) ⁱ 0.040($^{+62}_{-40}$) ^j		0.032 ^h	
$0 \rightarrow 4_2^+$	944	$E4$	16.5	0.083(16)			0.0017	
$0 \rightarrow 4_3^+$	2055	$E4$	0.6	0.0028(14)				
$0 \rightarrow 6_1^+$	548	$E6$	15.9	0.0072(20) ^b				
$0 \rightarrow 6_2^+$	1263	$E6$	20.8	0.015(4)				

^aThe errors shown in the parentheses are only due to the statistical errors in the cross section measurements and do not include any systematic errors due to model, cross correlations in deformation parameters, or reaction mechanism dependence.

^bThis transition has a negative value of matrix element.

^cReference 29. This value of $B(E2)$ is used to normalize the results of model calculations.

^dReference 5.

^eReference 23.

^fReference 30.

^gReference 31.

^hReference 32. This value of $B(E4)$ is used to normalize the results of the IBA model.

ⁱReference 33. The value refers to their analysis with the quantal corrections.

^jReference 34.

^kReference 3. (BM) Bohr-Mottelson model; the authors have used relative branching ratios and Q_0 of the ground state band for this result.

^lReference 4. (GGM) Gneuss-Greiner model, (GCM) general collective model, (RVM) rotation-vibrational model.

Table III shows the comparison of the present isoscalar $B(E3)$ values for the different 3^- states with the results obtained earlier from (d,d') experiments with 12 MeV deuterons²⁰ and Coulomb excitation with 14 MeV α particles.²³ The present isoscalar octupole strengths have been calculated using relation (4.7). It is evident from the table that our results for the 1633 and 1431 keV levels are in fairly good agreement with Coulomb excitation values, which gives some confidence in the present analysis. The $B(E3)$ values, except for the 1913 keV level, are in disagreement with the values derived earlier from (d,d') experiments. This, however, is not surprising, since the $B(E3)$ values derived from the earlier (d,d') experiments²⁰ are based on proportionality and a normalization, neither of which has been verified experimentally to a good approximation.

The sum of the $B(\text{IS},3)$ strength in ^{168}Er observed in the present experiment is $0.235 e^2 b^3$ or 20 s.p.u. and the centroid of this strength is at 1.907 MeV excitation energy. This can be compared with the nearby doubly closed shell

nucleus ^{146}Gd which has one known²⁶ 3^- state at 1.579 MeV with

$$B(E3;0 \rightarrow 3) = (0.33 \pm 0.04) e^2 b^3.$$

Relative to ^{146}Gd we have located in ^{168}Er 71% of the $l=3$ strength fractionated among several states with a centroid 328 keV higher in excitation energy.

Table III also includes theoretical predictions by Neergård and Vogel²⁷ based on the pairing plus modified octupole-octupole force residual interaction. Shown are the results for the quasiparticle random phase approximation, unperturbed (RPA) and perturbed by Coriolis coupling (CC). The results from the two calculations are similar except for the $K=1$, 1431 keV state, and there our result agrees better with the CC case, indicating the importance of Coriolis coupling in this nucleus.

For comparison with the IBA model, the following Hamiltonian was used to describe the negative parity states:

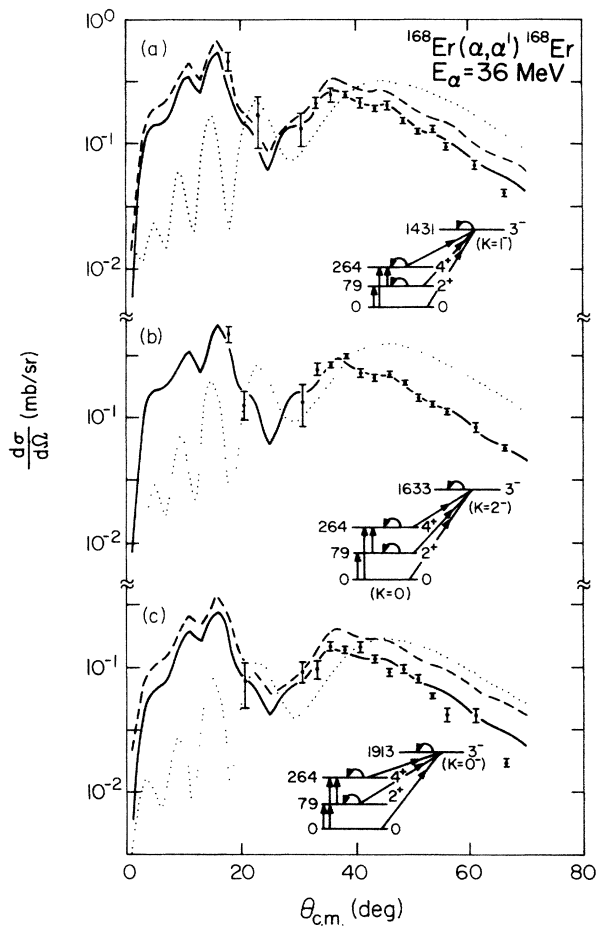


FIG. 7. (a) Experimental data and the coupled channel results for the 3^- (1431 keV, $K=1^-$) state. The full drawn curve is the coupled channel prediction as described in the text. The dashed curve is the prediction for which the $3^- \rightarrow 3^-$ coupling has been set to zero. The dotted curve is the one-step DWBA prediction for the same value of β_3 . (b) Same for the 3^- (1633 keV, $k=2^-$) state. (c) Same for the 3^- (1913 keV, $k=0^-$) state.

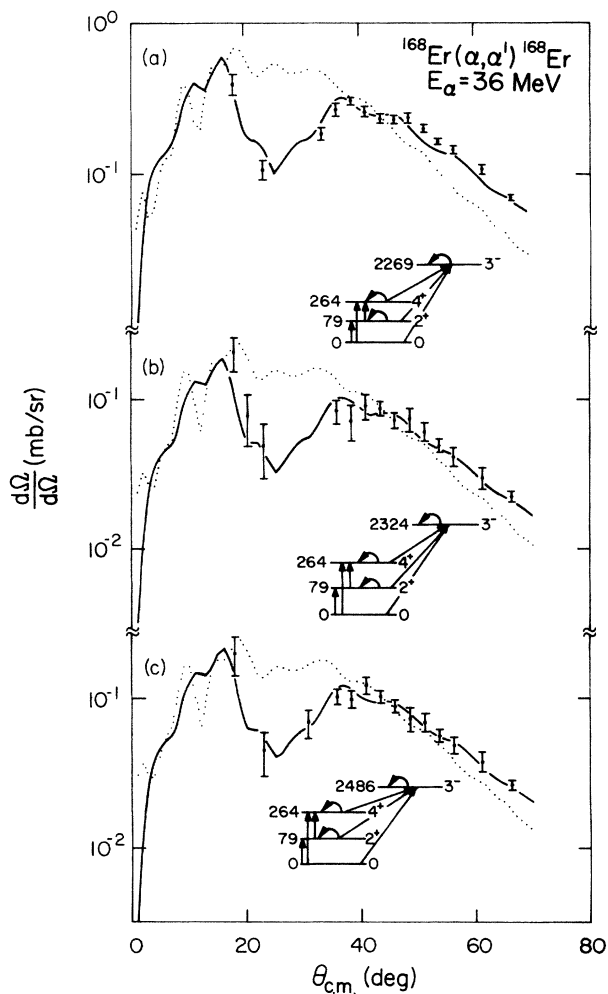


FIG. 8. (a) Experimental data and the coupled channel results for the 2269 keV state in the framework of octupole (solid curve) and quadrupole (dotted curve) vibration of an axially symmetric statically deformed nucleus with $\beta_2=0.23$. (b) Same for 2324 keV state. (c) Same for 2486 keV state.

ACKNOWLEDGMENTS

The authors wish to express their gratitude to Dr. O. Scholten, Dr. F. T. Baker, Dr. M. N. Harakeh, Dr. R. M.

Ronningen, Dr. A. S. Meigooni, Dr. C. Y. Wu, and Dr. P. Vogel for enlightening discussions of various aspects of this work. This research was supported by the National Science Foundation.

-
- *Present address: University of Warsaw, 00-681, Warsaw, Poland.
- †Present address: University of Uppsala, S-75121, Uppsala, Sweden.
- ‡Present address: Physical Research Institute, Leningrad State University, Petrodvoretz, Leningrad, U.S.S.R.
- ¹W. F. Davidson, D. D. Warner, R. F. Casten, K. Schreckenbach, H. G. Börner, J. Simic, M. Stojanovic, M. Bogdanovic, S. Koicki, W. Gelletly, G. R. Orr, and M. L. Stelts, *J. Phys. G* **7**, 455 (1981).
- ²D. D. Warner, R. F. Casten, and W. F. Davidson, *Phys. Rev. C* **24**, 1713 (1981).
- ³A. Bohr and B. R. Mottelson, *Phys. Scr.* **25**, 28 (1982).
- ⁴M. Seiwert, J. A. Maruhn, and P. O. Hess, *Phys. Rev. C* **30**, 1779 (1984).
- ⁵B. Kotlinski, Ph.D. thesis, University of Rochester, 1984.
- ⁶A. M. Bernstein, *Advances in Nuclear Physics*, edited by M. Baranger and E. Vogt (Plenum, New York, 1969), Vol. 3.
- ⁷J. Raynal, *Computing as a Language of Physics* (IAEA, Vienna, 1972).
- ⁸A. S. Davydov and G. F. Filippov, *Nucl. Phys.* **8**, 237 (1958).
- ⁹A. S. Davydov and V. S. Rostovsky, *Nucl. Phys.* **12**, 58 (1959).
- ¹⁰Taro Tamura, *Nucl. Phys.* **73**, 241 (1965).
- ¹¹Taro Tamura, *Rev. Mod. Phys.* **37**, 679 (1965).
- ¹²M. E. Rose, *Elementary Theory of Angular Momentum* (Wiley, New York, 1967), p. 61.
- ¹³L. W. Put and M. N. Harekh, *Phys. Lett.* **119B**, 253 (1982).
- ¹⁴M. J. A. de Voigt, D. Cline, and R. N. Horoshko, *Phys. Rev. C* **10**, 1798 (1974).
- ¹⁵L. W. Owen and G. R. Satchler, *Nucl. Phys.* **51**, 155 (1964).
- ¹⁶D. L. Hendrie, N. K. Glendenning, B. G. Harvey, O. N. Jarvis, H. H. Duhm, J. Saudinos, and J. Mahoney, *Phys. Lett.* **26B**, 127 (1968).
- ¹⁷W. W. Daehnick, J. D. Childs, and Z. Vrcelj, *Phys. Rev. C* **21**, 2253 (1980).
- ¹⁸I. M. Govil and H. W. Fulbright, *Bull. Am. Phys. Soc.* **29**, 719 (1984).
- ¹⁹T. Ichihara, H. Sakaguchi, M. Nakamura, T. Noro, F. Ohtani, H. Sakamoto, H. Ogawa, M. Yosoi, M. Ieiri, N. Isshiki, Y. Takeuchi, and S. Kobayashi, *Phys. Lett.* **149B**, 55 (1984).
- ²⁰P. O. Tjøm and B. Elbek, *Nucl. Phys.* **A107**, 385 (1968).
- ²¹W. Michaelis, H. Ottmar, and F. Weller, *Nucl. Phys.* **A150**, 161 (1970).
- ²²F. R. Metzger and V. K. Rasmussen, *Phys. Rev. C* **8**, 1099 (1973).
- ²³F. K. McGowan, W. T. Milner, R. L. Robinson, P. H. Stelson, and Z. W. Grabowski, *Nucl. Phys.* **A297**, 51 (1978).
- ²⁴G. Alaga, K. Alder, A. Bohr, and B. R. Mottelson, *K. Dan. Vidensk. Selsk. Mat.-Fys. Medd.* **29**, No. 9 (1955).
- ²⁵F. T. Baker, *Nucl. Phys.* **A299**, 357 (1978).
- ²⁶P. Kleinheinz, M. Ogawa, R. Broda, P. J. Daly, D. Haenni, H. Beuscher, and A. Kleinrahm, *Z. Phys. A* **286**, 27 (1978).
- ²⁷K. Neergård and P. Vogel, *Nucl. Phys.* **A145**, 33 (1970).
- ²⁸O. Scholten, Program Package, "PHINT" IBA-1 (unpublished).
- ²⁹L. M. Greenwood, *Nucl. Data Sheets* **11**, 385 (1974).
- ³⁰C. Baktash, J. X. Saladin, J. O'Brien, I. Y. Lee, and J. E. Holden, *Phys. Rev. C* **10**, 2265 (1974).
- ³¹J. M. Domingos, G. D. Symons, and A. C. Douglas, *Nucl. Phys.* **A180**, 600 (1972).
- ³²I. Y. Lee, J. X. Saladin, C. Baktash, J. E. Holden, and J. O'Brien, *Phys. Rev. Lett.* **33**, 383 (1974).
- ³³A. H. Shaw and J. S. Greenberg, *Phys. Rev. C* **10**, 263 (1974).
- ³⁴K. A. Erb, J. E. Holden, I. Y. Lee, J. X. Saladin, and T. K. Saylor, *Phys. Rev. Lett.* **29**, 1010 (1972).